

UK/02-02

Jan. 2002

## Finite Density Algorithm in Lattice QCD – a Canonical Ensemble Approach

Keh-Fei Liu\*

*Dept. of Physics and Astronomy, University of Kentucky, Lexington, KY 40506*

### Abstract

I will review the finite density algorithm for lattice QCD based on finite chemical potential and summarize the associated difficulties. I will propose a canonical ensemble approach which projects out the finite baryon number sector from the fermion determinant. For this algorithm to work, it requires an efficient method for calculating the fermion determinant and a Monte Carlo algorithm which accommodates unbiased estimate of the probability. I shall report on the progress made along this direction with the Padé -  $Z_2$  estimator of the determinant and its implementation in the newly developed Noisy Monte Carlo algorithm.

---

\*email: liu@pa.uky.edu

Invited talk at Nankai Symposium on Mathematical Physics, Tianjin, Oct. 2001 to be published in Journal of Modern Physics B.

# 1 Introduction

Fermions at finite density or finite chemical potential is a subject of a wide range of interest. It is relevant to condensed matter physics, such as the Hubbard model away from half-filling. The research about nuclei and neutron stars at low and high nucleon density is actively pursued in nuclear physics and astrophysics. The subject of quark gluon plasma is important for understanding the early universe and is being sought for in relativistic heavy-ion collisions in the laboratories. Furthermore, speculation about color superconducting phase has been proposed recently for quantum chromodynamics (QCD) at very high quark density [1].

Although there are models, e.g. chiral models and Nambu Jona-Lasinio model which have been used to study QCD at finite quark density, the only way to study QCD at finite density and temperature reliably and systematically is via lattice gauge calculations. There have been extensive lattice calculations of QCD at finite temperature [2]. On the contrary, the calculation at finite density is hampered by the lack of a viable algorithm.

In this talk, I shall first review the difficulties associated with the finite density algorithm with chemical potentials in Sec. 2. I will then outline in Sec. 3 a proposal for a finite density algorithm in the canonical ensemble which projects out the nonzero baryon number sector from the fermion determinant. In Sec. 4, a newly developed Noisy Monte Carlo algorithm which admits unbiased estimate of the probability is described. Its application to the fermion determinant is outlined in Sec. 5. I will discuss an efficient way, the Padé- $Z_2$  method, to estimate the  $Tr \log$  of the fermion matrix in Sec. 6. The recent progress on the implementation of the Kentucky Noisy Monte Carlo algorithm to dynamical fermions is presented in Sec. 7. Finally, a summary is given in Sec. 8.

## 2 Finite Chemical Potential

The usual approach to the finite density in the Euclidean path-integral formalism of lattice QCD is to consider the grand canonical ensemble with the partition function

$$Z_{GC}(\mu) = \sum_N Z_N e^{-\mu N} = \int \mathcal{D}U \det M[U, \mu] e^{-S_g[U]}, \quad (1)$$

where the fermion fields with fermion matrix  $M$  has been integrated to give the determinant.  $U$  is the gauge link variable and  $S_g$  is the gauge action. The chemical potential is introduced to the quark action with the  $e^{\mu a}$  factor in the time-forward hopping term and  $e^{-\mu a}$  in the time-backward hopping term. Here  $a$  is the lattice spacing. However, this causes the fermion action to be non-Hermitian, i.e.  $\gamma_5 M \gamma_5 \neq M$ . As a result, the fermion determinant  $\det M[U]$  is complex and this leads to the infamous sign problem.

There are several approaches to avoid the sign problem:

## 2.1 Fugacity Expansion

It was proposed by the Glasgow group [3] that the sign problem can be circumvented based on the expansion of the grand canonical partition function in powers of the fugacity variable  $e^{\mu/T}$ ,

$$Z_{GC}(\mu/T, T, V) = \sum_{B=-3V}^{B=3V} e^{\mu/T B} Z_B(T, V), \quad (2)$$

where  $Z_B$  is the canonical partition function for the baryon sector with baryon number  $B$ .  $Z_{GC}$  is calculated with reweighting of the fermion determinant

$$Z_{GC}(\mu) = \left\langle \frac{\det M[U, \mu]}{\det M[U, 0]} \right\rangle_{\mu=0}. \quad (3)$$

Since the reweighting is based on the gauge configuration with  $\mu = 0$ , it avoids the sign problem. However, this does not work, except perhaps at small  $\mu$  or near the finite temperature phase transition. We will dwell on this later in Sec. 3. This is caused by the ‘overlap problem’ [4] where the important samples of configurations in the  $\mu = 0$  simulation has exponentially small overlap with those relevant for the finite density. As a result, the onset of baryon begins at  $\mu \sim m_\pi/2$  instead of the expected  $M_N/3$  which resembles the situation of the quenched approximation.

## 2.2 Imaginary Chemical Potential

In this approach, the chemical potential is taking an imaginary value  $\mu = i\nu$ . The fermion determinant is real in this case and one can avoid the sign problem [5, 6, 7]. The partition function is

$$Z_{GC}(i\nu/T, T, V) = \text{Tr} e^{-\hat{H}/T} e^{i\nu \hat{B}/T}, \quad (4)$$

which is periodic with respect to  $\nu$  with a period of  $2\pi T$ . Comparing with Eq. (2), one can in principle obtain canonical partition function  $Z_B$  from the Fourier transform

$$Z_B(T, V) = \frac{1}{2\pi T} \int_0^{2\pi T} d\nu Z_{GC}(i\nu/T, T, V) e^{-i\nu B/T}. \quad (5)$$

In this approach, one needs to integrate over the whole range of  $\nu$  from 0 to  $2\pi T$  after one obtains the Monte Carlo configurations of  $Z_{GC}(i\nu/T, T, V)$  at different  $\nu$ . In practice, it is proposed to calculate the following ratio in the two-dimensional Hubbard model [7],

$$\frac{Z_{GC}(i\nu/T, T, V)}{Z_{GC}(i\nu_0/T, T, V)} = \int \mathcal{D}\phi e^{-S_{bos}} \frac{\det M(i\nu)}{\det M(i\nu_0)}, \quad (6)$$

with a reference value  $\nu_0$ . Several patches each centered around a different reference point  $\nu_0$  are used to cover the range of  $\nu$ . This was successful for the two-dimensional Hubbard model with a  $4^2 \times 10$  lattice up to  $B = 6$  where the determinant was calculated exactly. While this works for a small lattice in the Hubbard model, it would not work for reasonably large lattices in QCD. This is because the direct calculation of the determinant is a  $V^3$  (or  $V^2$  for a sparse matrix) operation which is an impracticable task for the quark matrix which is typically of the dimension  $10^6 \times 10^6$ . Any stochastic estimation of the determinant will inevitably introduce systematic error. Furthermore, this will also suffer from the ‘overlap’ problem discussed above. Any Monte Carlo simulation at a reference point  $\nu_0$  will have exponentially small overlap with those configurations important to a nonzero baryon density.

### 2.3 Overlap Ensuring Multi-parameter Reweighting

To alleviate the sign problem with the real chemical potential and the overlap problem due to reweighting, it is proposed [8] to do the reweighting in the multiple parameter space. The generic partition function  $Z_{GC}$  in Eq. (1) is parametrized by a set of parameters  $\alpha$ , such as the chemical potential  $\mu$ , the gauge coupling  $\beta$ , the quark mass  $m_q$ , etc. The partition function can be written to facilitate reweighting

$$Z_{GC}(\alpha) = \int \mathcal{D}U \det M[U, \alpha_0] e^{-S_g[U, \alpha_0]} \left\{ e^{-S_g[U, \alpha] + S_g[U, \alpha_0]} \frac{\det M[U, \alpha]}{\det M[U, \alpha_0]} \right\}, \quad (7)$$

where the Monte Carlo simulation is carried out with the  $\alpha_0$  set of parameters and the terms in the curly bracket are treated as observables. This is applied to study the end point in the  $T$ - $\mu$  phase diagram. In this case, the Monte Carlo simulation is carried out where the parameters in  $\alpha_0$  include  $\mu = 0$  and  $\beta_c$  which corresponds to the phase transition at temperature  $T_c$ . The parameter set  $\alpha$  in the reweighted measure include  $m_u \neq 0$  and an adjusted  $\beta$  in the gauge action. The new  $\beta$  is determined from the Lee-Yang zeros so that one is following the transition line in the  $T$ - $\mu$  plane and the large change in the determinant ratio in the reweighting is compensated by the change in the gauge action to ensure reasonable overlap. This is shown to work to locate the transition line from  $\mu = 0$  and  $T = T_c$  down to the critical point on the  $4^4$  and  $6^3 \times 4$  lattices with staggered fermions [8].

While the multi-parameter reweighting is successful near the transition line, it is not clear how to extend it beyond this region, particularly the  $T = 0$  case where one wants to keep the  $\beta$  and quark mass fixed while changing the  $\mu$ . One still expects to face the overlap problem in the latter case. For large volumes, calculating the determinant ratio will be subjected to the same practical difficulty as discussed in the previous section 2.2.

### 3 Finite Baryon Density – A Canonical Ensemble Approach

We would like to propose an algorithm to overcome the overlap problem at zero temperature which is based on the canonical ensemble approach. To avoid the overlap problem, one needs to lock in a definite nonzero baryon sector so that the exponentially large contamination from the zero-baryon sector is excluded. To see this, we first note that the fermion determinant is a superposition of multiple quark loops of all sizes and shapes. This can be easily seen from the property of the determinant

$$\det M = e^{Tr \log M} = 1 + \sum_{n=1} \frac{(Tr \log M)^n}{n!}. \quad (8)$$

Upon a hopping expansion of  $\log M$ ,  $Tr \log M$  represents a sum of single loops with all sizes and shapes. The determinant is then the sum of all multiple loops. The fermion loops can be separated into two classes. One is those which do not go across the time boundary and represent virtual quark-antiquark pairs; the other includes those which wraps around the time boundary which represent external quarks and antiquarks. The configuration with a baryon number one which entails three quark loops wrapping around the time boundary will have an energy  $M_B$  higher than that with zero baryon number. Thus, it is weighted with the probability  $e^{-M_B N_t a_t}$  compared with the one with no net baryons. We see from the above discussion that the fermion determinant contains a superposition of sectors of all baryon numbers, positive, negative and zero. At zero temperature where  $M_B N_t a_t \gg 1$ , the zero baryon sector dominates and all the other baryon sectors are exponentially suppressed. It is obvious that to avoid the overlap problem, one needs to select a definite nonzero baryon number sector and stay in it throughout the Markov chain of updating configurations. To select a particular baryon sector from the determinant can be achieved by the following procedure [9]: first, assign an  $U(1)$  phase factor  $e^{-i\phi}$  to the links between the time slices  $t$  and  $t+1$  so that the link  $U/U^\dagger$  is multiplied by  $e^{-i\phi}/e^{i\phi}$ ; then the particle number projection can be carried out through the Fourier transformation of the fermion determinant like in the BCS theory

$$P_N = \frac{1}{2\pi} \int_0^{2\pi} d\phi e^{-i\phi N} \det M[\phi] \quad (9)$$

where  $N$  is the net particle number, i.e. particle minus antiparticle. Note that all the virtual quark loops which do not reach the time boundary will have a net phase factor of unity; only those with a net  $N$  quark loops across the time boundary will have a phase factor  $e^{i\phi N}$  which can contribute to the integral in Eq. (9). Since QCD in canonical formulation does not break  $Z(3)$  symmetry, it is essential to take care that the ensemble is canonical with respect to triality. To this end, we shall consider the triality projection [9, 10] to the zero triality sector

$$\det_0 M = \frac{1}{3} \sum_{k=0,\pm 1} \det M[\phi + k2\pi/3]. \quad (10)$$

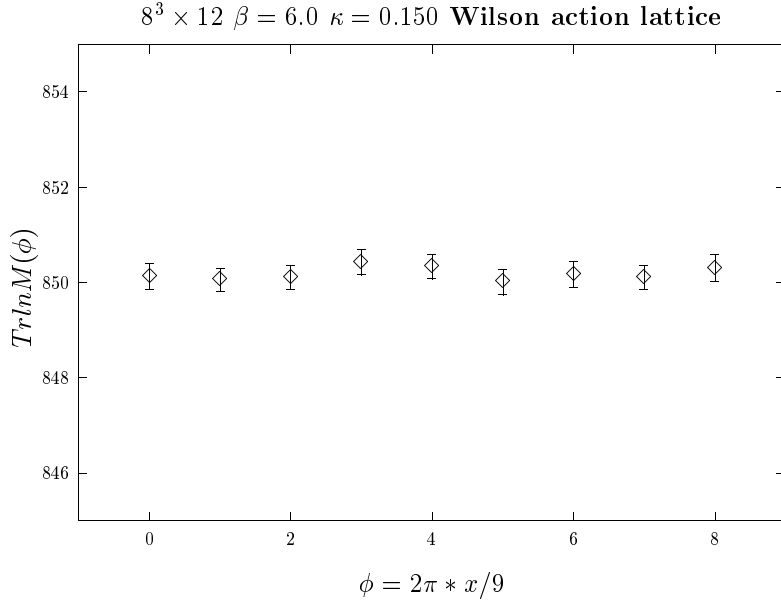


Figure 1:  $Tr \log M[\phi]$  for a  $8^3 \times 12$  configuration with Wilson action as a function of  $\phi$ .

This amounts to limiting the quark number  $N$  to a multiple of 3. Thus the triality zero sector corresponds to baryon sectors with integral baryon numbers.

Another essential ingredient to circumvent the overlap problem is to stay in the chosen nonzero baryon sector so as to avoid mixing with the zero baryon sector with exponentially large weight. This can be achieved by performing the baryon number projection as described above *before* the accept/reject step in the Monte Carlo updating of the gauge configuration. If this is not done, the accepted gauge configuration will be biased toward the zero baryon sector and it is very difficult to project out the nonzero baryon sector afterwards. This is analogous to the situation in the nuclear many-body theory where it is known [13] that the variation after projection (Zeh-Rouhaninejad-Yoccoz method [14, 15]) is superior than the variation before projection (Peierls-Yoccoz method [16]). The former gives the correct nuclear mass in the case of translation and yields much improved wave functions in mildly deformed nuclei than the latter.

To illustrate the overlap problem, we plot in Fig.1  $Tr \log M[\phi]$  for a configuration of the  $8^3 \times 12$  lattice with the Wilson action with  $\beta = 6.0$  and  $\kappa = 0.150$  which is obtained with 500  $Z_2$  noises. We see that it is rather flat in  $\phi$  indicating that the Fourier transform in Eq. (9) will mainly favor the zero baryon sector. On the other hand, at finite temperature, it is relatively easier for the quarks to be excited so that the zero baryon sector does not necessarily dominate other baryon sectors. Another way of seeing this is that the relative weighting factor  $e^{-M_B N_t a_t}$  can be  $O(1)$  at finite temperature. Thus, it should be easier to project out the nonzero baryon sector from the determinant. We plot in Fig. 2 a similarly obtained  $Tr \log M[\phi]$  for a

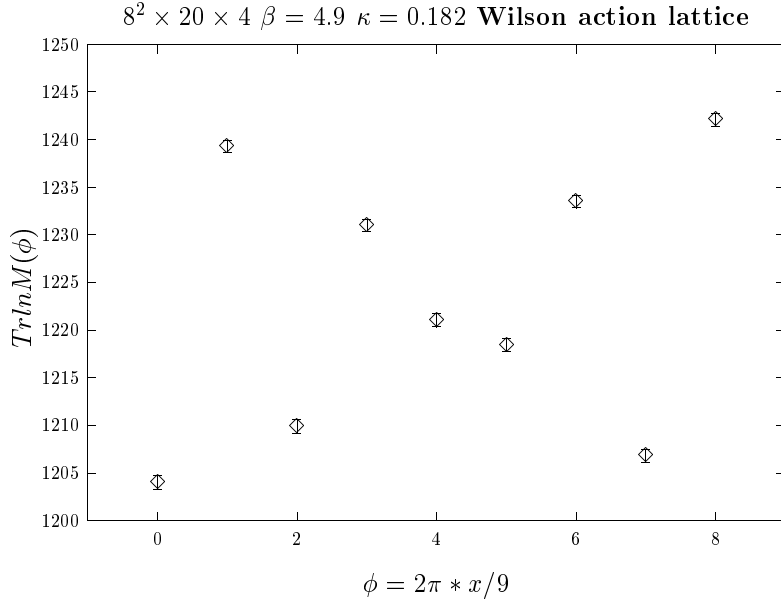


Figure 2:  $Tr \log M[\phi]$  for a  $8 \times 20^2 \times 4$  finite temperature configuration with dynamical fermion.

configuration of the  $8 \times 20^2 \times 4$  lattice with  $\beta = 4.9$  and  $\kappa = 0.182$ . We see from the figure that there is quite a bit of wiggling in this case as compared to that in Fig. 1 indicating that it is easier to project out a nonzero baryon sector through the Fourier transform at finite temperature.

We should mention that while we think we can overcome the overlap problem and the determinant  $\det M[\phi]$  is real in this approach, nevertheless in view of the fact that the Fourier transform in Eq. (9) involves the quark number  $N$  the canonical approach may still have the sign problem at the thermodynamic limit when  $N$  and  $V$  are very large. However, we think it might work for small  $N$  such as 3 or 6 for one or two baryons in a finite  $V$ . This should be a reasonable start for practical purposes.

While it is clear what the algorithm in the canonical approach entails, there are additional practical requirements for the algorithm to work. These include an unbiased estimation of the huge determinant in lattice QCD and, moreover, a Monte Carlo algorithm which accommodates the unbiased estimate of the probability. We shall discuss them in the following sections.

## 4 A Noisy Monte Carlo Algorithm

There are problems in physics which involve extensive quantities such as the fermion determinant which require  $V^3$  steps to compute exactly. Problems of this kind with large volumes are not numerically applicable with the usual Monte Carlo algorithm which require an exact evaluation of the probability ratios in the accept/reject step.

To address this problem, Kennedy and Kuti [11] proposed a Monte Carlo algorithm which admits stochastically estimated transition probabilities as long as they are unbiased. But there is a drawback. The probability could lie outside the interval between 0 and 1 since it is estimated stochastically. This probability bound violation will destroy detailed balance and lead to systematic bias. To control the probability violation with a large noise ensemble can be costly.

We propose a noisy Monte Carlo algorithm which avoids this difficulty with two Metropolis accept/reject steps. Let us consider a model with Hamiltonian  $H(U)$  where  $U$  collectively denotes the dynamical variables of the system. The major ingredient of the new approach is to transform the noise for the stochastic estimator into stochastic variables. The partition function of the model can be written as

$$\begin{aligned} Z &= \int [DU] e^{-H(U)} \\ &= \int [DU][D\xi] P_\xi(\xi) f(U, \xi). \end{aligned} \quad (11)$$

where  $f(U, \xi)$  is an unbiased estimator of  $e^{-H(U)}$  from the stochastic variable  $\xi$  and  $P_\xi$  is the probability distribution for  $\xi$ .

The next step is to address the lower probability-bound violation. One first notes that one can write the expectation value of the observable  $O$  as

$$\langle O \rangle = \int [DU][D\xi] P_\xi(\xi) O(U) \text{sign}(f) |f(U, \xi)| / Z, \quad (12)$$

where  $\text{sign}(f)$  is the sign of the function  $f$ . After redefining the partition function to be

$$Z = \int [DU][D\xi] P_\xi(\xi) |f(U, \xi)|, \quad (13)$$

which is semi-positive definite, the expectation of  $O$  in Eq. (12) can be rewritten as

$$\langle O \rangle = \langle O(U) \text{sign}(f) \rangle / \langle \text{sign}(f) \rangle. \quad (14)$$

As we see, the sign of  $f(U, \xi)$  is not a part of the probability any more but a part in the observable. Notice that this reinterpretation is possible because the sign of  $f(U, \xi)$  is a state function which depends on the configuration of  $U$  and  $\xi$ .

It is clear then, to avoid the problem of lower probability-bound violation, the accept/reject criterion has to be factorizable into a ratio of the new and old probabilities so that the sign of the estimated  $f(U, \xi)$  can be absorbed into the observable. This leads us to the Metropolis accept/reject criterion which incidentally cures the problem of upper probability-bound violation at the same time. It turns out two accept/reject steps are needed in general. The first one is to propose updating of  $U$  via some procedure while keeping the stochastic variables  $\xi$  fixed. The acceptance probability  $P_a$  is

$$P_a(U_1, \xi \rightarrow U_2, \xi) = \min\left(1, \frac{|f(U_2, \xi)|}{|f(U_1, \xi)|}\right). \quad (15)$$



The second accept/reject step involves the refreshing of the stochastic variables  $\xi$  according to the probability distribution  $P_\xi(\xi)$  while keeping  $U$  fixed. The acceptance probability is

$$P_a(U, \xi_1 \rightarrow U, \xi_2) = \min\left(1, \frac{|f(U, \xi_2)|}{|f(U, \xi_1)|}\right). \quad (16)$$

It is obvious that there is neither lower nor upper probability-bound violation in either of these two Metropolis accept/reject steps. Furthermore, it involves the ratios of separate state functions so that the sign of the stochastically estimated probability  $f(U, \xi)$  can be absorbed into the observable as in Eq. (14).

Detailed balance can be proven to be satisfied and it is unbiased [12]. Therefore, this is an exact algorithm.

## 5 Noisy Monte Carlo with Fermion Determinant

One immediate application of NMC is lattice QCD with dynamical fermions. The action is composed of two parts – the pure gauge action  $S_g(U)$  and a fermion action  $S_F(U) = -Tr \ln M(U)$ . Both are functionals of the gauge link variables  $U$ .

To find out the explicit form of  $f(U, \xi)$ , we note that the fermion determinant can be calculated stochastically as a random walk process [17]

$$e^{Tr \ln M} = 1 + Tr \ln M \left(1 + \frac{Tr \ln M}{2} \left(1 + \frac{Tr \ln M}{3} (\dots)\right)\right). \quad (17)$$

This can be expressed in the following integral

$$e^{Tr \ln M} = \int \prod_{i=1}^{\infty} d\eta_i P_\eta(\eta_i) \int_0^1 \prod_{n=2}^{\infty} d\rho_n \\ [1 + \eta_1^\dagger \ln M \eta_1 (1 + \theta(\rho_2 - \frac{1}{2}) \eta_2^\dagger \ln M \eta_2 (1 + \theta(\rho_3 - \frac{2}{3}) \eta_3^\dagger \ln M \eta_3 (\dots)], \quad (18)$$

where  $P_\eta(\eta_i)$  is the probability distribution for the stochastic variable  $\eta_i$ . It can be the Gaussian noise or the  $Z_2$  noise ( $P_\eta(\eta_i) = \delta(|\eta_i| - 1)$  in this case). The latter is preferred since it has the minimum variance [18].  $\rho_n$  is a stochastic variable with uniform distribution between 0 and 1. This sequence terminates stochastically in finite time and only the seeds from the pseudo-random number generator need to be stored in practice. The function  $f(U, \eta, \rho)$  ( $\xi$  in Eq. (11) is represented by two stochastic variables  $\eta$  and  $\rho$  here) is represented by the part of the integrand between the square brackets in Eq. (18). One can then use the efficient Padé- $Z_2$  algorithm [19] to calculate the  $\eta_i \ln M \eta_i$  in Eq. (18). We shall discuss this in the next section.

Finally, there is a practical concern that  $Tr \ln M$  can be large so that it takes a large statistics to have a reliable estimate of  $e^{Tr \ln M}$  from the series expansion in Eq. (18). In general, for the Taylor expansion  $e^x = \sum x^n/n!$ , the series will start to

converge when  $x^n/n! > x^{n+1}/(n+1)!$ . This happens at  $n = x$ . For the case  $x = 100$ , this implies that one needs to have more than  $100!$  stochastic configurations in the Monte Carlo integration in Eq. (18) in order to have a convergent estimate. Even then, the error bar will be very large. To avoid this difficulty, one can implement the following strategy. First, one notes that since the Metropolis accept/reject involves the ratio of exponentials, one can subtract a universal number  $x_0$  from the exponent  $x$  in the Taylor expansion without affecting the ratio. Second, one can use a specific form of the exponential to diminish the value of the exponent. In other words, one can replace  $e^x$  with  $(e^{(x-x_0)/N})^N$  to satisfy  $|x - x_0|/N < 1$ . The best choice for  $x_0$  is  $\bar{x}$ , the mean of  $x$ . In this case, the variance of  $e^x$  becomes  $e^{\delta^2/N} - 1$ .

## 6 The Padé – $\mathbf{Z}_2$ Method of Estimating Determinants

Now we shall discuss a very efficient way of estimating the fermion determinant stochastically [19].

### 6.1 Padé approximation

The starting point for the method is the Padé approximation of the logarithm function. The Padé approximant to  $\log(z)$  of order  $[K, K]$  at  $z_0$  is a rational function  $N(z)/D(z)$  where  $\deg N(z) = \deg D(z) = K$ , whose value and first  $2K$  derivatives agree with  $\log z$  at the specified point  $z_0$ . When the Padé approximant  $N(z)/D(z)$  is expressed in partial fractions, we obtain

$$\log z \approx b_0 + \sum_{k=1}^K \left( \frac{b_k}{z + c_k} \right), \quad (19)$$

whence it follows

$$\log \det \mathbf{M} = \text{Tr} \log \mathbf{M} \approx b_0 \text{Tr} \mathbf{I} + \sum_{k=1}^K b_k \cdot \text{Tr}(\mathbf{M} + c_k \mathbf{I})^{-1}. \quad (20)$$

The Padé approximation is not limited to the real axis. As long as the function is in the analytic domain, i. e. away from the cut of the log, say along the negative real axis, the Padé approximation can be made arbitrarily accurate by going to a higher order  $[K, K]$  and a judicious expansion point to cover the eigenvalue domain of the problem.

## 6.2 Complex $Z_2$ noise trace estimation

Exact computation of the trace inverse for  $N \times N$  matrices is very time consuming for matrices of size  $N \sim 10^6$ . However, the complex  $Z_2$  noise method has been shown to provide an efficient stochastic estimation of the trace [18, 20, 21]. In fact, it has been proved to be an optimal choice for the noise, producing a *minimum* variance [22].

The complex  $Z_2$  noise estimator can be briefly described as follows [18, 22]. We construct  $L$  noise vectors  $\eta^1, \eta^2, \dots, \eta^L$  where  $\eta^j = \{\eta_1^j, \eta_2^j, \eta_3^j, \dots, \eta_N^j\}^T$ , as follows. Each element  $\eta_n^j$  takes one of the four values  $\{\pm 1, \pm i\}$  chosen independently with equal probability. It follows from the statistics of  $\eta_n^j$  that

$$E[\langle \eta_n \rangle] \equiv E\left[\frac{1}{L} \sum_{j=1}^L \eta_n^j\right] = 0, \quad E[\langle \eta_m^\star \eta_n \rangle] \equiv E\left[\frac{1}{L} \sum_{j=1}^L \eta_m^{\star j} \eta_n^j\right] = \delta_{mn}. \quad (21)$$

The vectors can be used to construct an unbiased estimator for the trace inverse of a given matrix  $M$  as follows:

$$\begin{aligned} E[\langle \eta^\dagger M^{-1} \eta \rangle] &\equiv E\left[\frac{1}{L} \sum_{j=1}^L \sum_{m,n=1}^N \eta_m^{\star j} M_{m,n}^{-1} \eta_n^j\right] \\ &= \sum_n M_{n,n}^{-1} + \left(\sum_{m \neq n} M_{m,n}^{-1}\right) \left[\frac{1}{L} \sum_j \eta_m^{\star j} \eta_n^j\right] \\ &= \text{Tr } M^{-1}. \end{aligned}$$

The variance of the estimator is shown to be [22]

$$\begin{aligned} \sigma_M^2 &\equiv \text{Var}[\langle \eta^\dagger M^{-1} \eta \rangle] = E\left[|\langle \eta^\dagger M^{-1} \eta \rangle - \text{Tr } M^{-1}|^2\right] \\ &= \frac{1}{L} \sum_{m \neq n} M_{m,n}^{-1} (M_{m,n}^{-1})^\star = \frac{1}{L} \sum_{m \neq n} |M_{m,n}^{-1}|^2. \end{aligned}$$

The stochastic error of the complex  $Z_2$  noise estimate results only from the off-diagonal entries of the inverse matrix (the same is true for  $Z_n$  noise for any  $n$ ). However, other noises (such as Gaussian) have additional errors arising from diagonal entries. This is why the  $Z_2$  noise has minimum variance. For example, it has been demonstrated on a  $16^3 \times 24$  lattice with  $\beta = 6.0$  and  $\kappa = 0.148$  for the Wilson action that the  $Z_2$  noise standard deviation is smaller than that of the Gaussian noise by a factor of 1.54 [18].

Applying the complex  $Z_2$  estimator to the expression for the  $Tr \log M$  in Eq. (20), we find

$$\begin{aligned} &\sum_k b_k \text{Tr}(M + c_k)^{-1} \\ &\approx \frac{1}{L} \sum_k^K \sum_j^L b_k \eta^{j\dagger} (M + c_k)^{-1} \eta^j \end{aligned}$$

$$= \frac{1}{L} \sum_j^L \sum_{k=1}^K b_k \eta^{j\dagger} \xi^{k,j}, \quad (22)$$

where  $\xi^{k,j} = (M + c_k \mathbf{I})^{-1} \eta^j$  are the solutions of

$$(M + c_k \mathbf{I}) \xi^{k,j} = \eta^j, \quad (23)$$

Since  $M + c_k \mathbf{I}$  are shifted matrices with constant diagonal matrix elements, Eq. (23) can be solved collectively for all values of  $c_k$  within one iterative process by several algorithms, including the Quasi-Minimum Residual (QMR) [23], Multiple-Mass Minimum Residual ( $M^3$  R) [24], and GMRES[25]. We have adopted the  $M^3$  R algorithm, which has been shown to be about 2 times faster than the conjugate gradient algorithm, and the overhead for the multiple  $c_k$  is only 8% [26]. The only price to pay is memory: for each  $c_k$ , a vector of the solution needs to be stored. Furthermore, one observes that  $c_k > 0$ . This improves the conditioning of  $(\mathbf{M} + c_k \mathbf{I})$  since the eigenvalues of  $\mathbf{M}$  have positive real parts. Hence, we expect faster convergence for column inversions for Eq. (23).

In the next section, we describe a method which significantly reduces the stochastic error.

### 6.3 Improved PZ estimation with unbiased subtraction

In order to reduce the variance of the estimate, we introduce a suitably chosen set of traceless  $N \times N$  matrices  $\mathbf{Q}^{(p)}$ , i.e. which satisfy  $\sum_{n=1}^N \mathbf{Q}_{n,n}^{(p)} = 0$ ,  $p = 1 \cdots P$ . The expected value and variance for the modified estimator  $\langle \eta^\dagger (\mathbf{M}^{-1} - \sum_{p=1}^P \lambda_p \mathbf{Q}^{(p)}) \eta \rangle$  are given by

$$E[\langle \eta^\dagger (\mathbf{M}^{-1} - \sum_{p=1}^P \lambda_p \mathbf{Q}^{(p)}) \eta \rangle] = \text{Tr } \mathbf{M}^{-1}, \quad (24)$$

$$\Delta_M(\lambda) = \text{Var}[\langle \eta^\dagger (\mathbf{M}^{-1} - \sum_{p=1}^P \lambda_p \mathbf{Q}^{(p)}) \eta \rangle] = \frac{1}{L} \sum_{m \neq n} |\mathbf{M}_{m,n}^{-1} - \sum_{p=1}^P \lambda_p \mathbf{Q}_{m,n}^{(p)}|^2, \quad (25)$$

for any values of the real parameters  $\lambda_p$ . In other words, introducing the matrices  $\mathbf{Q}^{(p)}$  into the estimator produces no bias, but may reduce the error bars if the  $\mathbf{Q}^{(p)}$  are chosen judiciously. Further,  $\lambda_p$  may be varied at will to achieve a minimum variance estimate: this corresponds to a least-squares fit to the function  $\eta^\dagger \mathbf{M}^{-1} \eta$  sampled at points  $\eta_j$ ,  $j = 1 \cdots L$ , using the fitting functions  $\{1, \eta^\dagger \mathbf{Q}^{(p)} \eta\}$ ,  $p = 1 \cdots P$ .

We now turn to the question of choosing suitable traceless matrices  $\mathbf{Q}^{(p)}$  to use in the modified estimator. One possibility for the Wilson fermion matrix  $\mathbf{M} = \mathbf{I} - \kappa \mathbf{D}$  is suggested by the hopping parameter —  $\kappa$  expansion of the inverse matrix,

$$(\mathbf{M} + c_k \mathbf{I})^{-1} = \frac{1}{\mathbf{M} + c_k \mathbf{I}} = \frac{1}{(1 + c_k)(\mathbf{I} - \frac{\kappa}{(1+c_k)} \mathbf{D})}$$

$$= \frac{\mathbf{I}}{1 + c_k} + \frac{\kappa}{(1 + c_k)^2} \mathbf{D} + \frac{\kappa^2}{(1 + c_k)^3} \mathbf{D}^2 + \frac{\kappa^3}{(1 + c_k)^4} \mathbf{D}^3 + \cdots . \quad (26)$$

This suggests choosing the matrices  $\mathbf{Q}^{(p)}$  from among those matrices in the hopping parameter expansion which are traceless:

$$\begin{aligned} \mathbf{Q}^{(1)} &= \frac{\kappa}{(1 + c_k)^2} \mathbf{D}, \\ \mathbf{Q}^{(2)} &= \frac{\kappa^2}{(1 + c_k)^3} \mathbf{D}^2, \\ \mathbf{Q}^{(3)} &= \frac{\kappa^3}{(1 + c_k)^4} \mathbf{D}^3, \\ \mathbf{Q}^{(4)} &= \frac{\kappa^4}{(1 + c_k)^5} (\mathbf{D}^4 - \text{Tr} \mathbf{D}^4), \\ \mathbf{Q}^{(5)} &= \frac{\kappa^5}{(1 + c_k)^6} \mathbf{D}^5, \\ \mathbf{Q}^{(6)} &= \frac{\kappa^6}{(1 + c_k)^7} (\mathbf{D}^6 - \text{Tr} \mathbf{D}^6), \\ \mathbf{Q}^{(2r+1)} &= \frac{\kappa^{2r+1}}{(1 + c_k)^{2r+2}} \mathbf{D}^{2r+1}, \quad r = 3, 4, 5, \cdots . \end{aligned}$$

It may be verified that all of these matrices are traceless. In principle, one can include all the even powers which entails the explicit calculation of all the allowed loops in  $\text{Tr} \mathbf{D}^{2r}$ . In this manuscript we have only included  $\mathbf{Q}^{(4)}$ ,  $\mathbf{Q}^{(6)}$ , and  $\mathbf{Q}^{(2r+1)}$ .

## 6.4 Computation of $\text{Tr} \log M$

Our numerical computations were carried out with the Wilson action on the  $8^3 \times 12$  ( $N = 73728$ ) lattice with  $\beta = 5.6$ . We use the HMC with pseudofermions to generate gauge configurations. With a cold start, we obtain the fermion matrix  $\mathbf{M}_1$  after the plaquette becomes stable. The trajectories are traced with  $\tau = 0.01$  and 30 molecular dynamics steps using  $\kappa = 0.150$ .  $\mathbf{M}_2$  is then obtained from  $\mathbf{M}_1$  by an accepted trajectory run. Hence  $\mathbf{M}_1$  and  $\mathbf{M}_2$  differ by a continuum perturbation, and  $\log[\det \mathbf{M}_1 / \det \mathbf{M}_2] \sim \mathcal{O}(1)$ .

We first calculate  $\log \det \mathbf{M}_1$  with different orders of Padé expansion around  $z_0 = 0.1$  and  $z_0 = 1.0$ . We see from Table 1 that the 5th order Padé does not give the same answer for two different expansion points, suggesting that its accuracy is not sufficient for the range of eigenvalues of  $\mathbf{M}_1$ . Whereas, the 11th order Padé gives the same answer within errors. Thus, we shall choose  $\text{P}[11,11](z)$  with  $z_0 = 0.1$  to perform the calculations from this point on.

In Table 2, we give the results of improved estimations for  $\text{Tr} \log \mathbf{M}_1$ . We see that the variational technique described above can reduce the data fluctuations by more

Table 1: Unimproved and improved PZ estimates for  $\log [\det \mathbf{M}_1]$  with 100 complex  $\mathbf{Z}_2$  noise vectors.  $\kappa = 0.150$ .

$P[K, K](z)$	$K =$	5	7	9	11
$z_0 = 0.1$	Original:	473(10)	774(10)	796(10)	798(10)
	Improved:	487.25(62)	788.17(62)	810.83(62)	812.33(62)
$z_0 = 1.0$	Original:	798(10)	798(10)	798(10)	799(10)
	Improved:	812.60(62)	812.37(62)	812.36(62)	812.37(62)

Table 2: Central values for improved stochastic estimation of  $\log[\det \mathbf{M}_1]$  and  $r$ th-order improved Jackknife errors  $\delta_r$  are given for different numbers of  $\mathbf{Z}_2$  noise vectors.  $\kappa$  is 0.150 in this case.

# $\mathbf{Z}_2$	50	100	200	400	600	800	1000	3000	10000
$0^{th}$	802.98	797.98	810.97	816.78	815.89	813.10	816.53	813.15	812.81
$\delta_0$	$\pm 14.0$	$\pm 9.81$	$\pm 7.95$	$\pm 5.54$	$\pm 4.47$	$\pm 3.83$	$\pm 3.41$	$\pm 1.97$	$\pm 1.08$
$1^{st}$	807.89	811.21	814.13	815.11	814.01	814.62	814.97	—	—
$\delta_1$	$\pm 4.65$	$\pm 3.28$	$\pm 2.48$	$\pm 1.84$	$\pm 1.50$	$\pm 1.29$	$\pm 1.12$	-	-
$2^{nd}$	813.03	812.50	811.99	812.86	811.87	812.89	813.04	—	—
$\delta_2$	$\pm 2.46$	$\pm 1.65$	$\pm 1.34$	$\pm 1.01$	$\pm 0.83$	$\pm 0.72$	$\pm 0.64$	-	-
$3^{rd}$	812.07	812.01	811.79	812.44	812.18	812.99	813.03	—	—
$\delta_3$	$\pm 1.88$	$\pm 1.31$	$\pm 1.01$	$\pm 0.74$	$\pm 0.58$	$\pm 0.51$	$\pm 0.44$	-	-
$4^{th}$	812.28	812.52	812.57	812.86	812.85	813.25	813.40	—	—
$\delta_4$	$\pm 1.20$	$\pm 0.94$	$\pm 0.68$	$\pm 0.48$	$\pm 0.39$	$\pm 0.35$	$\pm 0.30$	-	-
$5^{th}$	813.50	813.07	813.36	813.70	813.47	813.54	813.50	—	—
$\delta_5$	$\pm 0.82$	$\pm 0.62$	$\pm 0.47$	$\pm 0.34$	$\pm 0.29$	$\pm 0.25$	$\pm 0.22$	-	-
$6^{ts}$	813.54	813.23	813.22	813.28	813.20	813.37	813.26	—	—
$\delta_6$	$\pm 0.67$	$\pm 0.49$	$\pm 0.35$	$\pm 0.25$	$\pm 0.21$	$\pm 0.18$	$\pm 0.16$	-	-
$7^{ts}$	814.18	813.74	813.44	813.42	813.39	—	—	—	—
$\delta_7$	$\pm 0.44$	$\pm 0.36$	$\pm 0.26$	$\pm 0.19$	$\pm 0.16$	-	-	-	-
$9^{th}$	813.77	813.62	813.49	813.40	813.43	—	—	—	—
$\delta_9$	$\pm 0.40$	$\pm 0.30$	$\pm 0.22$	$\pm 0.16$	$\pm 0.14$	-	-	-	-
$11^{th}$	813.54	813.41	813.45	813.44	813.43	—	—	—	—
$\delta_{11}$	$\pm 0.38$	$\pm 0.27$	$\pm 0.21$	$\pm 0.15$	$\pm 0.13$	-	-	-	-

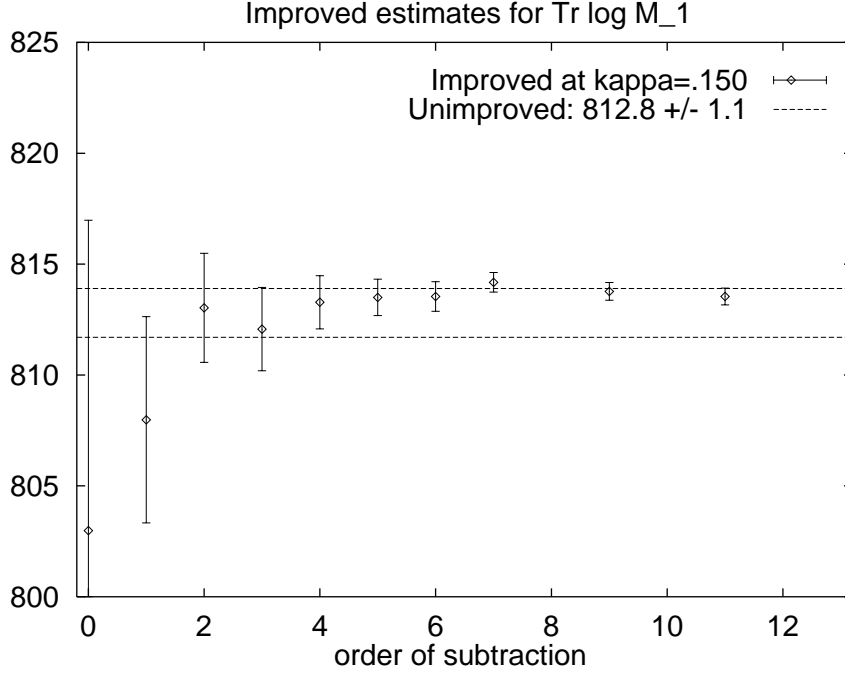


Figure 3: The improved PZ estimate of  $\text{Tr log } \mathbf{M}_1$  with 50 noises as a function of the order of subtraction and compared to that of unimproved estimate with 10,000 noises. The dashed lines are drawn with a distance of  $1 \sigma$  away from the central value of the unimproved estimate.

than an order of magnitude. For example, the unimproved error  $\delta_0 = 5.54$  in Table 2 for 400  $Z_2$  noises is reduced to  $\delta_{11} = 0.15$  for the subtraction which includes up to the  $\mathbf{Q}^{11}$  matrix. This is 37 times smaller. Comparing the central values in the last row (i.e. the 11<sup>th</sup> order improved) with that of unimproved estimate with 10,000  $Z_2$  noises, we see that they are the same within errors. This verifies that the variational subtraction scheme that we employed does not introduce biased errors. The improved estimates of  $\text{Tr log } \mathbf{M}_1$  from 50  $Z_2$  noises with errors  $\delta_r$  from Table 2 are plotted in comparison with the central value of the unimproved estimate from 10,000 noises in Fig. 3.

## 7 Implementation of the Kentucky Noisy Monte Carlo Algorithm

We have recently implemented the above Noisy Monte Carlo algorithm to the simulation of lattice QCD with dynamical fermions by incorporating the full determinant directly [28]. Our algorithm uses pure gauge field updating with a shifted gauge coupling to minimize fluctuations in the trace log is the Wilson Dirac matrix. It gives the correct results as compared to the standard Hybrid Monte Carlo simulation. However,

the present simulation has a low acceptance rate due to the pure gauge update and results in long autocorrelations. We are in the process of working out an alternative updating scheme with molecular dynamics trajectory to include the feedback of the determinantal effects on the gauge field which should be more efficient than the pure gauge update.

## 8 Summary

After reviewing the finite density algorithm for QCD with the chemical potential, we propose a canonical approach by projecting out the definite baryon number sector from the fermion determinant and stay in the sector throughout the Monte Carlo updating. This should circumvent the overlap problem. In order to make the algorithm practical, one needs an efficient way to estimate the huge fermion determinant and a Monte Carlo algorithm which admits unbiased estimates of the probability without upper unitarity bound violations. These are achieved with the Padé- $Z_2$  estimate of the determinant and the Noisy Monte Carlo algorithm. So far, we have implemented the Kentucky Noisy Monte Carlo algorithm to incorporate dynamical fermions in QCD on a relatively small lattice and medium heavy quark based on pure gauge updating. As a next step, we will work on a more efficient updating algorithm and project out the baryon sector to see if the finite density algorithm proposed here will live up to its promise.

## Acknowledgments

This work is partially supported by the U.S. DOE grant DE-FG05-84ER40154. The author wishes to thank M. Faber for introducing the subject of the finite density to him and Shao-Jing Dong for providing some unpublished figures. Fruitful discussions with M. Alford, I. Barbour, U.-J. Wiese, and R. Sugar are acknowledged. He would also thank the organizer, Ge Mo-lin for the invitation to attend the conference and his hospitality.

## References

- [1] M. Alford, K. Rajagopal, and F. Wilczek, *Phys. Lett.* **B422**, 247 (1998); R. Rapp, T. Schaefer, E.V. Shuryak, and M. Velkovsky, *Phys. Rev. Lett.* **81**, 53 (1998); for a review, see for example, K. Rajagopal and F. Wilczek, hep-ph/0011333.
- [2] For recent review, see S. Ejiri, *Nucl. Phys. B (Proc. Suppl.)* **94**, 19 (2001).



- [3] I. M. Barbour, S. E. Morrison, E. G. Klepfish, J. B. Kogut, and M.-P. Lombardo, *Nucl. Phys. (Proc. Suppl.)* **60A**, 220 (1998); I.M. Barbour, C.T.H. Davies, and Z. Sabeur, *Phys. Lett.* **B215**, 567 (1988).
- [4] M. Alford, *Nucl. Phys. B (Proc. Suppl.)* **73**, 161 (1999).
- [5] E. Dagotto, A. Moreo, R. Sugar, and D. Toussaint, *Phys. Rev.* **B41**, 811 (1990).
- [6] N. Weiss, *Phys. Rev.* **D35**, 2495 (1987); A. Hasenfratz and D. Toussaint, *Nucl. Phys.* **B371**, 539 (1992).
- [7] M. Alford, A. Kapustin, and F. Wilczek, *Phys. Rev.* **D59**, 054502 (2000).
- [8] Z. Fodor and S.D. Katz, hep-lat/0104001; JHEP 0203, 014 (2002) [hep-lat/0106002].
- [9] M. Faber, *Nucl. Phys.* **B444**, 563 (1995) and private communication.
- [10] M. Faber, O. Borisenko, S. Mashkevich, and G. Zinovjev, *Nucl. Phys. B(Proc. Suppl.)* **42**, 484 (1995).
- [11] A.D. Kennedy, J. Kuti, *Phys. Rev. Lett.* **54** (1985) 2473.
- [12] L. Lin, K. F. Liu, and J. Sloan, *Phys. Rev.* **D61**, 074505 (2000), [hep-lat/9905033].
- [13] For reviews on the subject see for example C.W. Wong, *Phys. Rep.* **15C**, 285 (1975); D.J. Rowe, Nuclear Collective Motion, Methuen (1970); P. Ring and P. Schuck, The Nuclear Many-Body Problem, Springer-Verlag (1980).
- [14] H.D. Zeh, *Z. Phys.* **188**, 361 (1965).
- [15] H. Rouhaninejad and J. Yoccoz, *Nucl. Phys.* **78**, 353 (1966).
- [16] R.E. Peierls and J. Yoccoz, *Proc. Phys. Soc. (London)* **A70**, 381 (1957).
- [17] G. Bhanot, A. D. Kennedy, *Phys. Lett.* **157B**, 70 (1985).
- [18] S. J. Dong and K. F. Liu, *Phys. Lett.* **B 328**, 130 (1994).
- [19] C. Thron, S. J. Dong, K. F. Liu, H. P. Ying, *Phys. Rev.* **D57**, 1642 (1998).
- [20] S.J. Dong, J.-F. Lagaë, and K.F. Liu, *Phys. Rev. Lett.* **75**, 2096 (1995); S.J. Dong, J.-F. Lagaë, and K.F. Liu, *Phys. Rev.* **D54**, 5496 (1996).
- [21] N. Eicker, *et al*, SESAM-Collaboration, *Phys. Lett.* **B389**, 720 (1996).
- [22] S. Bernardson, P. McCarty and C. Thron, *Comp. Phys. Commun.* **78**, 256 (1994).

- [23] A. Frommer, B. Nöckel, S. Güsken, Th. Lippert and K. Schilling, *Int. J. Mod. Phys.* **C6**, 627 (1995).
- [24] U. Glässner, S. Güsken, Th. Lippert, G. Ritzenhöfer, K. Schilling, and A. Frommer, hep-lat/9605008.
- [25] A. Frommer and U. Glässner, Wuppertal preprint BUGHW-SC96/8, to appear in SIAM J. Scientific Computing.
- [26] He-Ping Ying, S.J. Dong and K.F. Liu, *Nucl. Phys.* **B**(proc. Suppl.) **53**, 993 (1997).
- [27] S. Duane, A. D. Kennedy, B. J. Pendleton, D. Roweth, *Phys. Lett.* **B195** (1987) 216.
- [28] B. Joó, I. Horváth, and K.F. Liu, hep-lat/0112033.